Research Article

INTERNATIONAL JOURNAL OF ADVANCED ROBOTIC SYSTEMS

International Journal of Advanced Robotic Systems
March-April 2017: 1–10

DOI: 10.1177/1729881417699147
journals.sagepub.com/home/arx
SAGE

Lateral control strategy for a hypersonic cruise missile

Yonghua Fan, Pengpeng Yan, Hongyang Xu and Fan Wang

Abstract

Hypersonic cruise missile always adopts the configuration of waverider body with the restraint of scramjet. As a result, the lateral motion exhibits serious coupling, and the controller design of the lateral lateral system cannot be conducted separately for yaw channel and roll channel. A multiple input and multiple output optimal control method with integrators is presented to design the lateral combined control system for hypersonic cruise missile. A hypersonic cruise missile lateral model is linearized as a multiple input and multiple output plant, which is coupled by kinematics and fin deflection between yaw and roll. In lateral combined controller, the integrators are augmented, respectively, into the loop of roll angle and lateral overload to ensure that the commands are tracked with zero steady-state error. Through simulation, the proposed controller demonstrates good performance in tracking the command of roll angle and lateral overload.

Keywords

Hypersonic cruise missile, lateral combined control, integrate optimal control

Date received: 11 June 2016; accepted: 20 February 2017

Topic: Special Issue - Control of Hypersonic Flight Vehicles
Topic Editor: Danwei Wang
Associate Editor: Bin Xu

Introduction

With the breakthrough of the scramjet and heat safeguard, the hypersonic vehicle has tended to develop into cruise missile to realize global strike.[1–7] Many projects of hypersonic cruise missile (HCM) such as High-Speed Strike Weapon programs and Hypersonic Air-breathing Weapon Concept, which are being managed by the US Air Force Research Lab and Defense Advanced Research Programs Agency, have been carried out.[8]

Over several past decades, a large number of researches have been focused on hypersonic aircraft aerodynamic modeling,[9–11] because hypersonic vehicle has a character of highly areo-propulsion integrated configuration. Consequently, it is difficult to measure and estimate the aerodynamic parameters and set an accurate model. Also, the scramjet is highly sensitive to the vehicle flying conditions such as angle of attack and sliding angle. Many works have been concentrated on designing high-precision control system to guarantee that the scramjet works efficiently. The uncertainties in the dynamic model, such as aerodynamic, thermodynamic, and elastic coupling, are considered as the primary disturbances. Matthew[12] reported an adaptive linear quadratic altitude and velocity tracking control algorithm for the longitudinal model of a generic air-breathing hypersonic flight vehicle. In case of input saturation, dead-zone input nonlinearity, states constraint, and actuator fault, the reader can refer to the studies of Xu et al.[13–16] A nonlinear controller for an air-breathing hypersonic

School of Astronautics, Northwestern Polytechnic University, Xi'an, Shaanxi, China

Corresponding author:
Yonghua Fan, Flight Control Research Institute, School of Astronautics, Northwestern Polytechnic University, No.127, YouYi West Rode, BeiLin District, Xi'an, Shaanxi 710072, China.
Email: fyhlixin@163.com

vehicle was designed by Fiorentini et al.[17] Xu et al.[18] presented an adaptive sliding mode control for hypersonic aircraft with nonlinear and model uncertainty. Considering the effect of a digital computer on board with a certain sampling interval, the control system for an HCM using discrete sliding model is proposed by Fan et al.[19] Xu et al.[20–23] have studied the dynamic surface control with neural network to deal with the system uncertainty using minimal-learning-parameter technique and global tracking design.

The researchers are mainly focused on the longitudinal controller design for hypersonic vehicle, and only a very few are focused on the lateral controller.[24,25] The lateral controller design is more difficult than the longitudinal. As in many published papers, the height and velocity are usually controlled in longitudinal autopilot; nonetheless, they are also in the same channel. However, there is serious coupling between yaw and roll due to the surface symmetrical configuration. The lateral autopilot should control the yaw channel and roll channel simultaneously. Also, the desirable control performance cannot be got if the lateral system is designed separately as yaw and roll. In addition, the lateral model of hypersonic aircraft can be seldom studied in literatures, since the lateral model is more complicated.

In this article, a lateral control strategy for an HCM is proposed. Firstly, an HCM's lateral model is established and the aerodynamic force and moment coefficients are given. Then, the HCM's lateral model is linearized as a multiple input and multiple output (MIMO) plant by small perturbation linear method. Based on the MIMOs optimal control theory, the lateral combined control system is designed. To ensure that the commands are tracked with zero steady-state error, the integrators are augmented, respectively, into the loop of roll angle and lateral acceleration. It is proved by simulation results that the proposed controller demonstrates good performance in tracking the command of roll angle and lateral acceleration, even when the serious couple exists in the lateral model.

This article is organized as follows: The dynamics and discrete model of HCM is given in "The lateral aerodynamic model of HCM" section. The design of lateral combined controller is illustrated in "The optimal controller with integrator" section. Then, we conduct simulations and give the results to demonstrate the reasonability of our design. Finally, we make a conclusion in the last section.

The lateral aerodynamic model of HCM

HCM has waverider configuration with an under-fuselage scramjet inlet. The asymmetrical aerodynamic configuration is shown as Figure 1.

HCM has four control surfaces: two outward canted vertical tails are used for yaw control and a pair of horizontal elevators is applied for pitch and roll control. The equations of lateral motion are

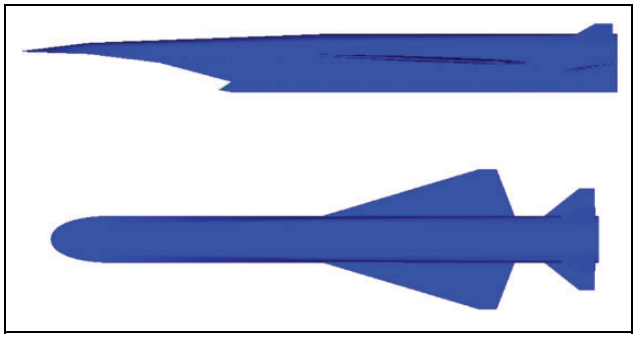

Figure 1. The aerodynamic configuration of HCM.
HCM: hypersonic cruise missile.

$$
\begin{aligned}
&\dot{\psi}_v = -\frac{Z}{mV\cos\gamma}\\
&J_x\dot{\omega}_x - J_{xy}\dot{\omega}_y = M_x\\
&J_y\dot{\omega}_y - J_{xy}\dot{\omega}_x = M_y\\
&\dot{\psi} = \omega_y\\
&\psi = \psi_v + \beta\\
&Z = \frac{1}{2}\rho V^2 S C_z\\
&M_x = \frac{1}{2}\rho V^2 S\bar{c} C m_x\\
&M_y = \frac{1}{2}\rho V^2 S\bar{c} C m_y
\end{aligned}
\tag{1}
$$

where C_z is the lateral force coefficient; Cm_x and Cm_y are the rolling moment coefficient and the yawing moment coefficient, respectively; ψ_v is the trajectory heading angle; γ is the flight-path angle; β is the sideslip angle; and ψ is the yaw angle.

The force and moment coefficients of lateral motion are as follows

$$
\begin{aligned}
C\,Z =& -0.06575\beta + 0.0009247\alpha\cdot\beta - 0.004419Ma\cdot\beta\\
&- 0.004567\cdot\delta_y + 0.00009495\alpha\cdot\delta_y + 0.0003589Ma\cdot\delta_y\\
Cm_x =& -0.001793\beta - 0.0003893\alpha\cdot\beta + 0.0002058Ma\cdot\beta\\
&- 0.001654\delta_x - 0.00008671\alpha\cdot\delta_x + 0.00008738Ma\cdot\delta_x\\
&- 0.0008569\delta_y - 0.00001917\alpha\cdot\delta_y + 0.00006509Ma\cdot\delta_y\\
&- 0.0818\cdot\bar{\omega}_x - 0.0121\cdot\bar{\omega}_y\\
Cm_y =& -0.001645\beta - 0.0002077\alpha\cdot\beta + 0.0002251Ma\cdot\beta\\
&- 0.00137\delta_y + 0.00002618\alpha\cdot\delta_y + 0.0001069Ma\cdot\delta_y\\
&- 0.1363\cdot\bar{\omega}_y - 0.0090\cdot\bar{\omega}_x
\end{aligned}
\tag{2}
$$

where α is the angle of attack, β is the sideslip angle, δ_x is the aileron, and δ_y is the rudder. $\bar{\omega}_x$ and $\bar{\omega}_y$ represent the nondimensional factors of rotational angular rate. The formulas of $\bar{\omega}_x$ and $\bar{\omega}_y$ are

$$\bar{\omega}_x = \frac{L_{\text{ref}}}{2V}\omega_x,\ \bar{\omega}_y = \frac{L_{\text{ref}}}{2V}\omega_y \tag{3}$$

where L_{ref} denotes the reference length, and V is the flight speed.

By using the method of coefficient frozen, the lateral motion equations of HCM can be linearized

$$\begin{cases} \dfrac{d\omega_x}{dt} + b_{11}\omega_x + b_{14}\beta + b_{12}\omega_y = -b_{18}\delta_x - b_{17}\delta_y \\ \dfrac{d\omega_y}{dt} + b_{22}\omega_y + b_{24}\beta + b_{21}\omega_x = -b_{27}\delta_y \\ \dfrac{d\beta}{dt} + b_{34}\beta + \omega_y + b_{35}\gamma = -b_{37}\delta_y \\ \dfrac{d\gamma}{dt} = \omega_x \\ \dfrac{d\psi}{dt} = \omega_y \\ \psi - \psi_V - \beta = 0 \end{cases} \tag{4}$$

The dynamic coefficients in equation (4) are

$$b_{11} = -\frac{M_x^{\omega_x}}{J_x},\ b_{12} = -\frac{M_x^{\omega_y}}{J_x},\ b_{14} = -\frac{M_x^{\beta}}{J_x},\ b_{21} = -\frac{M_y^{\omega_x}}{J_y}$$

$$b_{22} = -\frac{M_y^{\omega_y}}{J_y},\ b_{24} = -\frac{M_y^{\beta}}{J_y},\ b_{34} = \frac{P - Z^{\beta}}{mV},\ b_{35} = -\frac{g}{V}\cos\vartheta$$

The control coefficients in equation (4) are

$$b_{18} = -\frac{M_x^{\delta_x}}{J_x},\ b_{19} = -\frac{M_x^{\delta_y}}{J_x},\ b_{27} = -\frac{M_y^{\delta_y}}{J_y},\ b_{37} = -\frac{Z^{\delta_y}}{mV}$$

In equation (2), the roll moment coefficients Cm_x contain the yaw motion coupling parameters such as the sideslip angle β, rudder δ_y, and the rotational angular rate of yaw ω_y, which denotes the yaw motion, will affect the roll response. In equation (4), the coefficients b_{14}, b_{12} and b_{17} indicate the coupling in roll which is caused by yaw channel. Conversely, b_{21} and b_{35} are the coupling caused by roll.

Rewriting the above equations into the form of state space, we have

$$\begin{cases} \dot{x} = Ax + Bu \\ y = Cx + Du \\ z = Hx + Lu \end{cases} \tag{5}$$

where $x = [\omega_x \quad \omega_y \quad \beta \quad \gamma]^T$ is the state vector,. So please check throughout the article and edit accordingly.] $u = [\delta_x \quad \delta_y]^T$ is the control vector, $y = [\gamma \quad n_z \quad \omega_x \quad \omega_y]^T$ is the output vector, and $z = [\gamma \quad n_z]^T$ is the first two lines of y. The coefficient matrixes of the system are

$$A = \begin{bmatrix} -b_{11} & -b_{12} & -b_{14} & 0 \\ -b_{21} & -b_{22} & -b_{24} & 0 \\ 0 & -1 & -b_{34} & -b_{35} \\ 1 & 0 & 0 & 0 \end{bmatrix},\ B = \begin{bmatrix} -b_{18} & -b_{17} \\ 0 & -b_{27} \\ 0 & -b_{37} \\ 0 & 0 \end{bmatrix}$$

$$C = \begin{bmatrix} 0 & 0 & 0 & 1 \\ 0 & 0 & -\dfrac{Vb_{34}}{g} & 0 \\ 1 & 0 & 0 & 0 \\ 0 & 1 & 0 & 0 \end{bmatrix},\ D = \begin{bmatrix} 0 & 0 \\ 0 & -\dfrac{Vb_{37}}{g} \\ 0 & 0 \\ 0 & 0 \end{bmatrix}$$

$$H = C\begin{pmatrix} 1,: \\ 2,: \end{pmatrix},\ L = D\begin{pmatrix} 1,: \\ 2,: \end{pmatrix} \tag{6}$$

The optimal controller with integrator

The design of control system can be transformed as the "standard" linear quadratic regulator (LQR) problem

$$\min J = \int_0^{\infty} (z^T Q z + u^T R u) dt \tag{7}$$

Subject to the dynamics

$$\dot{x} = Ax + Bu \tag{8}$$

$$y = Cx + Du \tag{9}$$

$$z = Hx \tag{10}$$

We can get the optimal state feedback is

$$u = -R^{-1}B^T P x = -Kx \tag{11}$$

where P is the solution to the algebraic Riccati equation

$$A^T P + PA - PBR^{-1}B^T P + H^T Q H = 0 \tag{12}$$

The optimal state feedback can be transformed as output feedback with equation (9)

$$u = -Kx = -[I - KC^{-1}D]^{-1}KC^{-1}y \tag{13}$$

Clearly, the LQR problem has no integrator which will cause the steady error. Also, the control fin is proportion to the track error; as a result, the fin will move with a large rate. So we can penalize the control rate instead of the fin deflection. The cost function is

$$\min J = \int_0^{\infty} \left(z^T Q z + \dot{u}^T R \dot{u}\right) dt \tag{14}$$

Let

$$\dot{u} = v \tag{15}$$

The cost function can be written as

$$\min J = \int_0^\infty \left(z^T Q z + v^T R v\right) dt \tag{16}$$

The state equation can be augment

$$\begin{bmatrix} \dot{x} \\ \dot{u} \end{bmatrix} = \begin{bmatrix} A & B \\ 0 & 0 \end{bmatrix} \begin{bmatrix} x \\ u \end{bmatrix} + \begin{bmatrix} 0 \\ 1 \end{bmatrix} v \tag{17}$$

Let $\bar{X} = [x \quad u]^T$. Using equation (13), we can get the optimal feedback

$$\dot{u} = v = -K\bar{X} = -\bar{K}y \tag{18}$$

where $\bar{K} = [I - KC^{-1}D]^{-1}KC^{-1}$.

By integrating both side of equation (18), we can get

$$u = -\bar{K}\int y \tag{19}$$

The aim of the lateral control system of HCM is to keep yaw channel stable by using overload feedback control and to achieve lateral maneuver through roll angle tracking control. That is to say, the purpose of the control system is to ensure roll angle $\gamma \to \gamma_c$ and lateral overload $n_z \to n_{zc}$.

So we choose the cost function

$$\min J = \int_0^\infty \left\{ \begin{bmatrix} \gamma - K_{s11}\gamma_c \\ n_z - K_{s22}n_{zc} \end{bmatrix}^T \begin{bmatrix} Q_{11} & 0 \\ 0 & Q_{22} \end{bmatrix} \begin{bmatrix} \gamma - K_{s11}\gamma_c \\ n_z - K_{s22}n_{zc} \end{bmatrix} + \begin{bmatrix} \dot{\delta}_x \\ \dot{\delta}_y \end{bmatrix}^T \begin{bmatrix} R_{11} & 0 \\ 0 & R_{22} \end{bmatrix} \begin{bmatrix} \dot{\delta}_x \\ \dot{\delta}_y \end{bmatrix} \right\} dt \tag{20}$$

where the positive definite matrix Q_1 is error weighting matrix, and $Q_1 = \begin{bmatrix} Q_{11} & 0 \\ 0 & Q_{22} \end{bmatrix}$. The positive definite matrix R_1 is control weight matrix, and $R_1 = \begin{bmatrix} R_{11} & 0 \\ 0 & R_{22} \end{bmatrix}$. K_{s11} and K_{s22} represent the forward gains of the control command. $\dot{\delta}_x$ and $\dot{\delta}_y$ denote the rates of control vector.

To introduce the integrator, the δ_x and δ_y be augmented as new states, using the $\dot{\delta}_x$ and $\dot{\delta}_y$ as control vector and augmenting the $\dot{\omega}_x$ and $\dot{\omega}_y$ as new outputs. We can get the augmented state-space equation

$$\begin{cases} \dot{x}_1 = A_1 x_1 + B_1 u_1 \\ y_1 = C_1 x_1 + D_1 u_1 \\ z_1 = H_1 x_1 + L_1 u_1 \end{cases} \tag{21}$$

where

$$\boldsymbol{x}_1 = [\omega_x \quad \omega_y \quad \beta \quad \gamma \quad \delta_x \quad \delta_y]^T, u_1 = [\dot{\delta}_x \quad \dot{\delta}_y]^T,$$

$$y_1 = [\gamma \quad n_z \quad \omega_x \quad \omega_y \quad \dot{\omega}_x \quad \dot{\omega}_y]^T, z_1 = y_1 \begin{pmatrix} 1,: \\ 2,: \end{pmatrix},$$

$$H_1 = C_1 \begin{pmatrix} 1,: \\ 2,: \end{pmatrix}, L_1 = D_1 \begin{pmatrix} 1,: \\ 2,: \end{pmatrix}$$

$$A_1 = \begin{bmatrix} -b_{11} & -b_{12} & -b_{14} & 0 & -b_{18} & -b_{17} \\ -b_{21} & -b_{22} & -b_{24} & 0 & 0 & -b_{27} \\ 0 & -1 & -b_{34} & -b_{35} & 0 & -b_{37} \\ 1 & 0 & 0 & 0 & 0 & 0 \\ 0 & 0 & 0 & 0 & 0 & 0 \\ 0 & 0 & 0 & 0 & 0 & 0 \end{bmatrix}, \quad B_1 = \begin{bmatrix} 0 & 0 \\ 0 & 0 \\ 0 & 0 \\ 0 & 0 \\ 1 & 0 \\ 0 & 1 \end{bmatrix},$$

$$C_1 = \begin{bmatrix} 0 & 0 & 0 & 1 & 0 & 0 \\ 0 & 0 & -\frac{Vb_{34}}{g} & 0 & 0 & -\frac{Vb_{37}}{g} \\ 1 & 0 & 0 & 0 & 0 & 0 \\ 0 & 1 & 0 & 0 & 0 & 0 \\ -b_{11} & -b_{12} & -b_{14} & 0 & -b_{18} & -b_{17} \\ -b_{21} & -b_{22} & -b_{24} & 0 & 0 & -b_{27} \end{bmatrix}, \quad D_1 = \begin{bmatrix} 0 & 0 \\ 0 & 0 \\ 0 & 0 \\ 0 & 0 \\ 0 & 0 \\ 0 & 0 \end{bmatrix}$$

D_1 is zero, and therefore, $y_1 = C_1 x_1$. Then, let $y_2 = x_2 = y_1 = C_1 x_1$. Equation (6) can be rewritten as

$$\begin{cases} \dot{x}_2 = A_2 x_2 + B_2 u_1 \\ y_2 = C_2 x_2 \\ z_2 = H_2 x_2 \end{cases} \tag{22}$$

where

$$x_2 = y_2 = [\gamma \quad n_z \quad \omega_x \quad \omega_y \quad \dot{\omega}_x \quad \dot{\omega}_y]^T, z_2 = [\gamma \quad n_z]^T,$$

$$A_2 = C_1 A_1 C_1^{-1}, B_2 = C_1 B_1, C_2 = I, H_2 = C_2 \begin{pmatrix} 1,: \\ 2,: \end{pmatrix}$$

By introducing roll angle command γ_c and lateral overload command n_{zc} into the state-space equation, we can get the state space model of command tracking that

$$\begin{cases} \dot{x}_2 = A_2 x_2 + B_2 u_1 \\ \tilde{y}_2 = C_2 x_2 - K_s [\gamma_c \quad n_{zc}]^T \\ \tilde{z}_2 = H_2 x_2 - K_s [\gamma_c \quad n_{zc}]^T \end{cases} \tag{23}$$

where K_{s11} and K_{s22} represent the forward gains of the control command

$$K_s = \begin{bmatrix} K_{s11} & 0 \\ 0 & K_{s22} \end{bmatrix}, K_s = \begin{bmatrix} K_{s11} & 0 \\ 0 & K_{s22} \\ 0 & 0 \\ 0 & 0 \\ 0 & 0 \\ 0 & 0 \end{bmatrix}$$

$$\tilde{y}_2 = [\gamma - K_{s11}\gamma_c \quad n_z - K_{s22}n_{zc} \quad \omega_x \quad \omega_y \quad \dot{\omega}_x \quad \dot{\omega}_y]^T$$

$$\tilde{z}_2 = [\gamma - K_{s11}\gamma_c \quad n_z - K_{s22}n_{zc}]^T$$

Equations (20) and (23) are a standard LQR problem. So we have transformed the optimal tracking problem to

a regular problem. By solving the Riccati equation (24), we have

$$A_2^T P + PA_2 - PB_2 R^{-1} B_2{}^T P + Q_2 = 0 \tag{24}$$

where $Q_2 = (C_1^{-1})^T H_1^T Q_1 H_1 C_1^{-1}$.

We can obtain the optimal control law

$$u_1 = \begin{bmatrix} \dot{\delta}_x \\ \dot{\delta}_y \end{bmatrix} = -Kx_2 \tag{25}$$

In equation (25), $K = R^{-1} B_2{}^T P$, and P is the solution of equation (24).

By transforming the state feedback to output feedback, the optimal control law is easily denoted as

$$u_1 = -(I - KC_2{}^{-1} D_2)^{-1} KC_2{}^{-1} \tilde{y}_2 \tag{26}$$

where $C_2 = I$, $D_2 = 0$, and the optimal control law is

$$u_1 = -K\tilde{y}_2 \tag{27}$$

By integrating both side of the equation (27), one can yield the optimal control commands

$$u = \begin{bmatrix} \delta_x \\ \delta_y \end{bmatrix} = -K \begin{bmatrix} \int (\gamma - K_{s11}\gamma_c)dt \\ \int (n_z - K_{s22} n_{zc})dt \\ \int \omega_x dt \\ \int \omega_y dt \\ \omega_x \\ \omega_y \end{bmatrix} = -K \begin{bmatrix} \int (\gamma - K_{s11}\gamma_c)dt \\ \int (n_z - K_{s22} n_{zc})dt \\ \gamma \\ \psi \\ \omega_x \\ \omega_y \end{bmatrix} \tag{28}$$

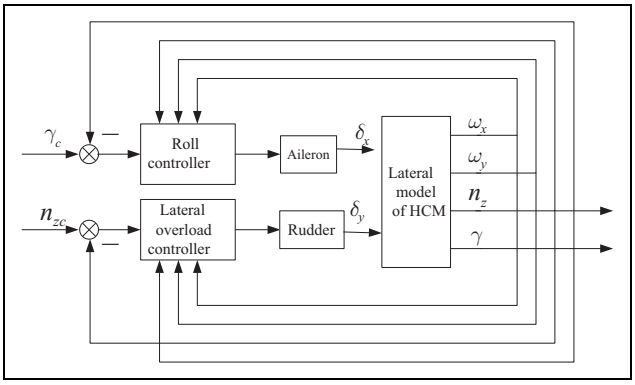

Figure 2. The structure of lateral control system of HCM.
HCM: hypersonic cruise missile.

where $K_s = (-C_c A_c{}^{-1} B'_c)^{-1}$, and the formulas of A_c, B_c, and C_c are as documented in the study of Mracek and Ridgely.[26]

Consequently, the structure of lateral control system of HCM is shown in Figure 2.

Simulation

Assuming the missile cruise at height $H = 23$ km and Mach number $\mathrm{Ma} = 5$, the parameter matrixes of state space equations are as follows

$$A_1 = \begin{bmatrix} -50.424 & -7.4588 & 416.4347 & 0 & -926.3487 & -450.407 \\ -0.1845 & -2.794 & -18.8738 & 0 & 0 & -29.2377 \\ 0 & 1 & -0.2266 & -0.0067 & 0 & -0.0219 \\ 1 & 0 & 0 & 0 & 0 & 0 \\ 0 & 0 & 0 & 0 & 0 & 0 \\ 0 & 0 & 0 & 0 & 0 & 0 \end{bmatrix}$$

$$C_1 = \begin{bmatrix} 0 & 0 & 0 & 1 & 0 & 0 \\ 0 & 0 & -26.8638 & 0 & 0 & -2.5965 \\ 1 & 0 & 0 & 0 & 0 & 0 \\ 0 & 1 & 0 & 0 & 0 & 0 \\ -50.424 & -7.4588 & 416.4347 & 0 & -926.3487 & -450.407 \\ -0.1845 & -2.794 & -18.8738 & 0 & 0 & -29.2377 \end{bmatrix}, \quad B_1 = \begin{bmatrix} 0 & 0 \\ 0 & 0 \\ 0 & 0 \\ 0 & 0 \\ 1 & 0 \\ 0 & 1 \end{bmatrix}, \quad D_1 = \begin{bmatrix} 0 & 0 \\ 0 & 0 \\ 0 & 0 \\ 0 & 0 \\ 0 & 0 \\ 0 & 0 \end{bmatrix}$$

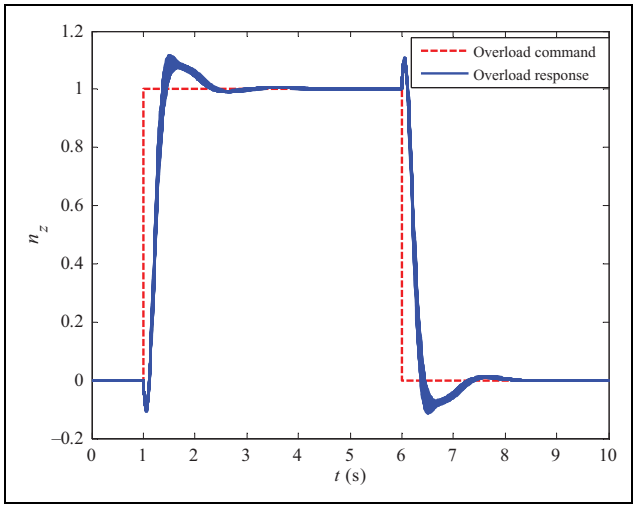

Figure 3. Results of lateral overload.

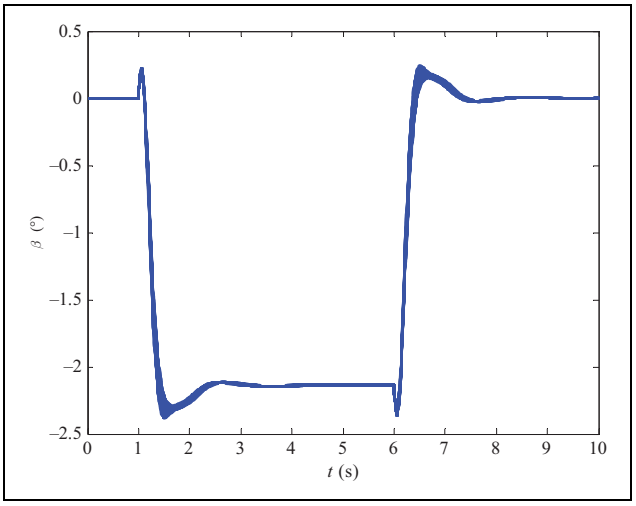

Figure 4. Results of sideslip angle.

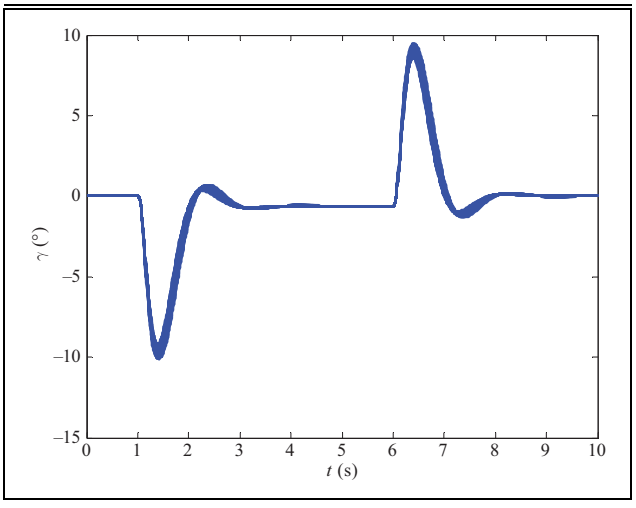

Figure 5. Results of roll angle.

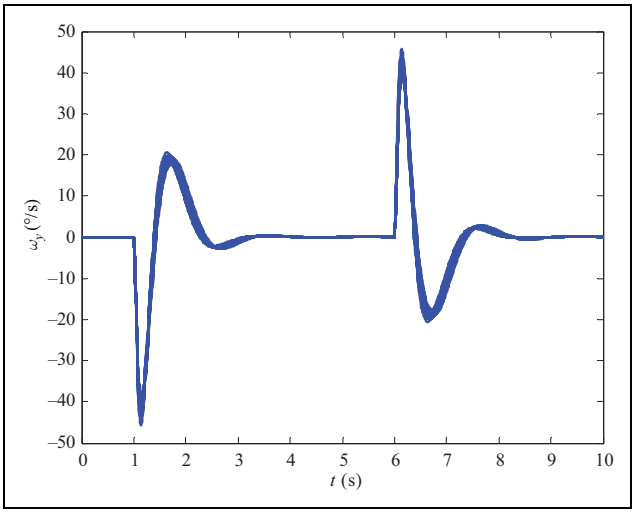

Figure 6. Results of roll rate.

Chose weighted matrixes Q and R of linear quadratic cost function as

$$Q = \begin{bmatrix} 5 & 0 \\ 0 & 2 \end{bmatrix}$$
$$R = \begin{bmatrix} 4 & 0 \\ 0 & 1 \end{bmatrix} \tag{29}$$

According to equation (26), we can get the gain matrices K and K_s

$$K = \begin{bmatrix} -1.085 & 0.1660 & -0.3516 & 0.5581 & -0.007 & 0.1214 \\ -0.5397 & -1.3119 & -0.1294 & -7.1731 & -0.0001 & -0.7172 \end{bmatrix}$$

$$K_s = \begin{bmatrix} 1 & 0 \\ 0 & 1.0451 \end{bmatrix}$$

To validate the robustness of controller, the uncertainties of the model are considered as $|\Delta m| \leq 0.03$, $|\Delta S| \leq 0.03$, $|\Delta J_x| \leq 0.05$, $|\Delta J_y| \leq 0.05$, $|\Delta C_z| \leq 0.10$, $|\Delta Cm_x| \leq 0.10$, $|\Delta Cm_y| \leq 0.10$, and $|\Delta q| \leq 0.05$. Slide to turn (STT) and bank to turn (BTT) are taken into account as two typical simulation conditions. The Monte Carlo simulation results of 100 times are shown as follows.

1) *STT simulation.* Let $\gamma_c = 0$, and n_{zc} is unit square wave signal from 1 s to 5 s; the simulation results of the lateral control system of HCM are shown in Figures 3 to 9.

Simulation results show that the lateral combined control system can track the roll angle command and lateral overload command with zero steady-state error. However, under this condition, it means that the lateral overload is obtained by the sideslip angle which is called STT. While tracking 1 g lateral overload command, the missile will introduce the sideslip about $-2.4°$. Although sideslip angle

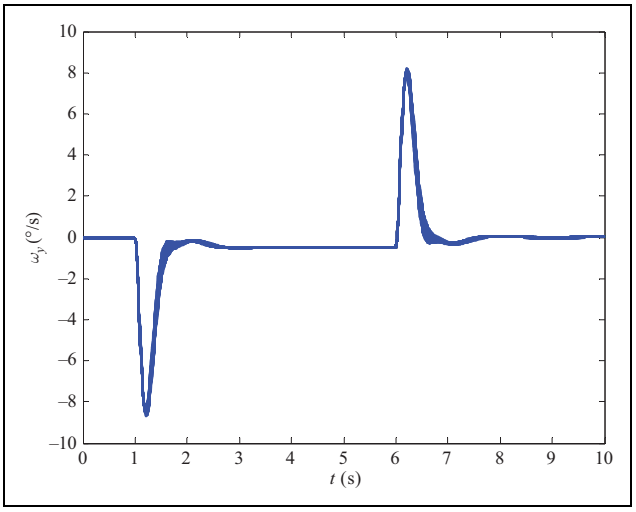

Figure 7. Results of yaw rate.

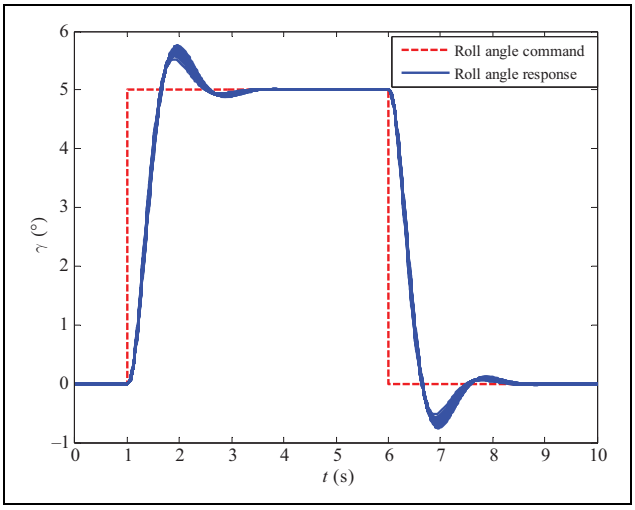

Figure 10. Results of roll angle.

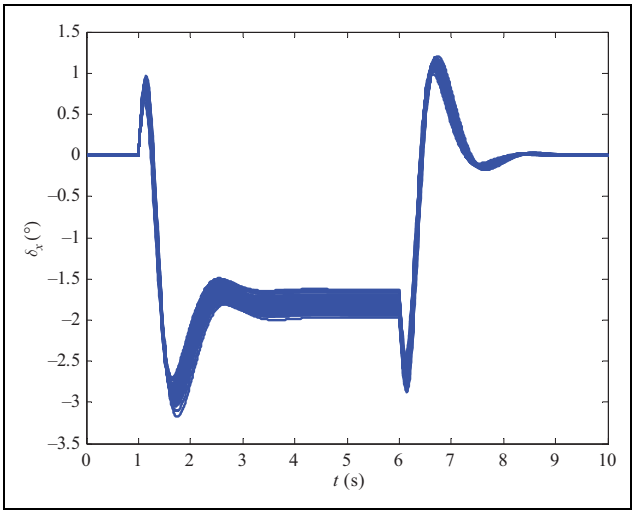

Figure 8. Results of aileron.

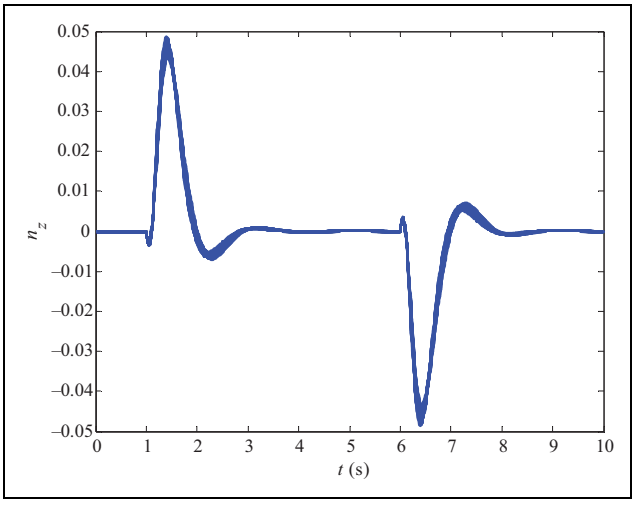

Figure 11. Results of lateral overload.

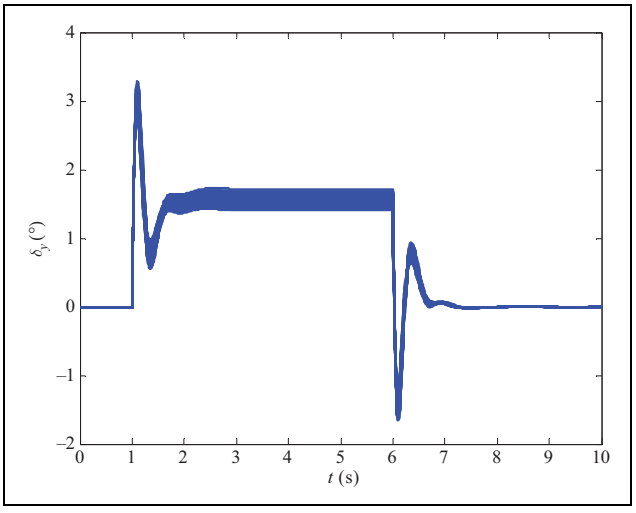

Figure 9. Results of rudder.

is not larger, it can also cause intense coupling in roll, as shown in Figures 5 and 6. The amplitude of roll is disturbed up to 9.7°, and the roll rate is up to 47° /s. Therefore, the lateral maneuver using STT cannot be applied for HCM; it should use the method of BTT, which achieves the lateral maneuver by controlling the roll to change the direction of lift which can be seen as follows.

2) *BTT simulation.* Let $n_{zc} = 0$, and γ_c is a square wave signal from 1 s to 5s. The simulation results of the lateral control system of HCM are shown in Figures 10 to 16.

Under this condition, the lateral maneuver is called BTT; in this mode, the purpose of yaw with feedback of lateral overload n_z is only to augment the stability, and therefore, $n_{zc} = 0$. The lateral maneuver is achieved by rolling the body to change the direction of lift as in airplane.

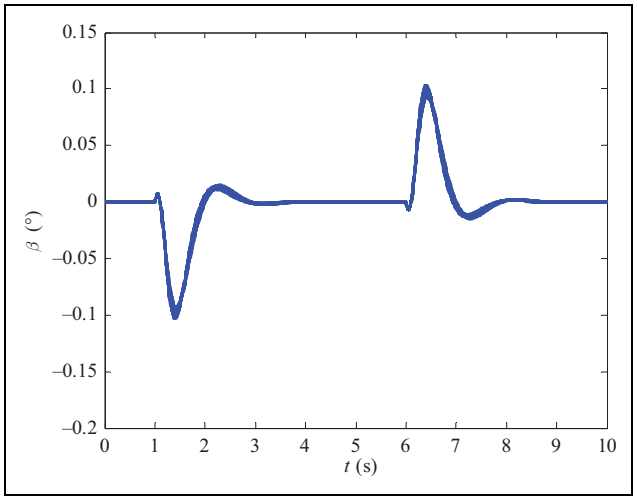

Figure 12. Results of sideslip angle.

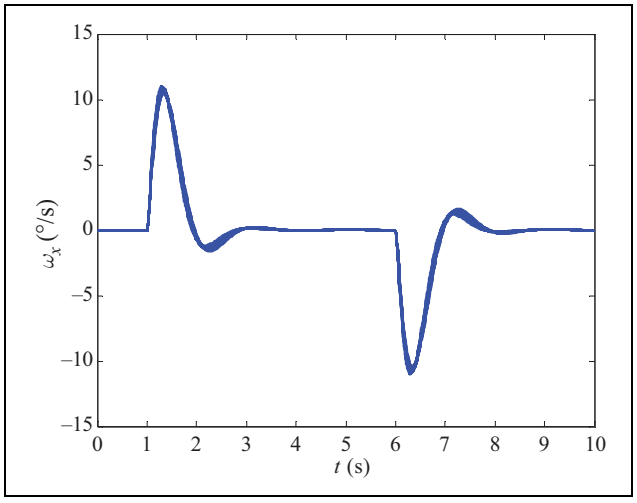

Figure 13. Results of roll rate.

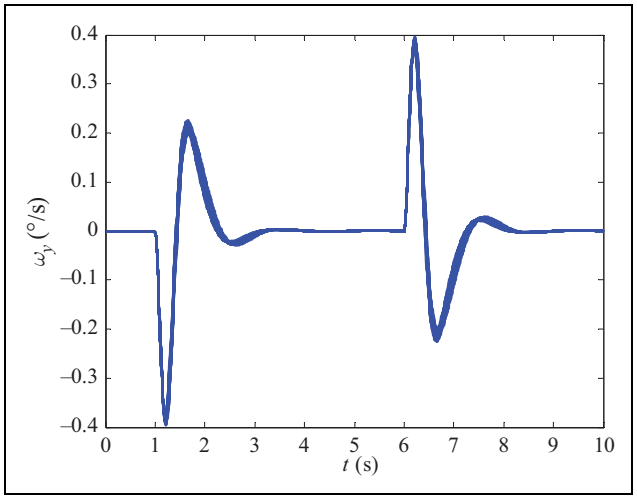

Figure 14. Results of yaw rate.

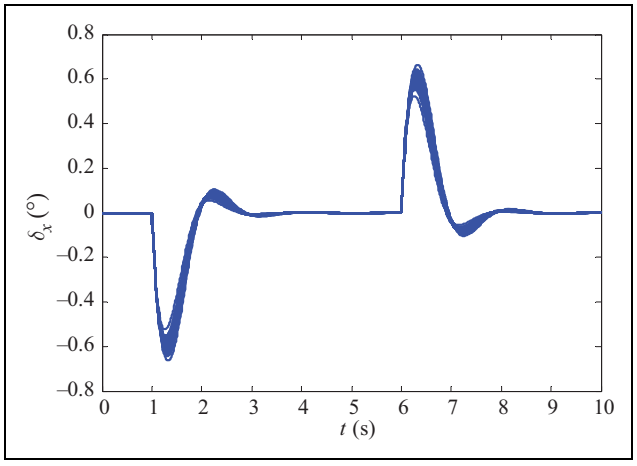

Figure 15. Results of aileron.

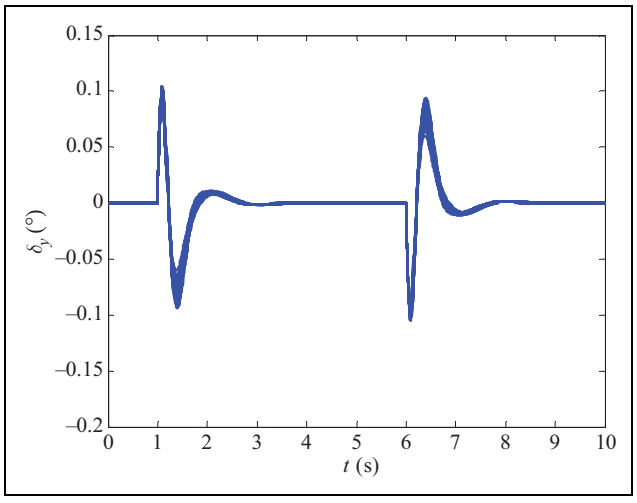

Figure 16. Results of rudder.

With the simulations, it is also proved that the lateral control system has desirable performance of tracking roll and lateral overload command, respectively, as shown in Figures 10 and 11. The controller has quickly tracked the roll command; the rise time of roll is about 0.5 s. Nevertheless, in this condition, the effects of coupling in lateral are more insignificant. As shown in Figures 12 and 14, the lateral overload caused by the roll motion is only 0.05 g, and the yaw rate is about 0.4° /s. The simulations can also show that it is very efficient by using the lateral maneuver mode of BTT, which can decrease the coupling between the yaw and roll greatly.

Conclusion

In this article, a lateral combined control system is designed by using MIMO optimal method for HCM with strong coupling in lateral model. In the controller, integrators are augmented to achieve no steady error. Simulation results demonstrate that the control system has good performance

in tracking roll angle command and yaw overload command, even when the strong coupling exists in the model.

Declaration of conflicting interests

The author(s) declared no potential conflicts of interest with respect to the research, authorship, and/or publication of this article.

Funding

The author(s) disclosed receipt of the following financial support for the research, authorship, and/or publication of this article: This paper is supported by Fundamental Research Funds for the Central Universities under grant no. 3102015BJ008, Aeronautical Science Foundation of China under grant no. 2015ZA53003, Natural Science Basic Research Plan in Shaanxi Province (2014JQ8326, 2015JM6272, 2016KJXX-86), and Fundamental Research Funds of Shenzhen Science and Technology Project (JCYJ20160229172341417), and this work is also supported by the Special Science Research Foundation of Doctor Subject for Higher education under grant no. 20136102120012.

References

1. Xu B and Shi Z. An overview on flight dynamics and control approaches for hypersonic vehicles. *Sci China Inf Sci* 2015; 58(7): 1–19.
2. Ferguson F, Dasque N, Mrema HF, et al. A coupled aerodynamic and propulsive performance analysis of a generic hypersonic vehicle. In: *The 51st AIAA/SAE/ASEE joint propulsion conference, propulsion and energy forum*, Orlando, FL, 27–29 July 2015.
3. Wiese DP, Annaswamy AM, Muse JA, et al. Adaptive output feedback based on closed-loop reference models for hypersonic vehicles. *J Guid Control Dynam* 2015; 38(12): 2429–2440.
4. Mehta SS, Ton C and MacKunis W. Acceleration-free nonlinear guidance and tracking control of hypersonic missiles for maximum target penetration. In: *AIAA guidance, navigation, and control conference*, San Diego, CA, USA, 4–8 January 2016.
5. Starkey R, Liu D, Baldelli D, et al. Rapid conceptual design and analysis of a hypersonic air-breathing missile. In: *15th AIAA international space planes and hypersonic systems and technologies conference*, Dayton, OH, April 28–1 May 2008, p. 2590.
6. Yu P, Shtessel YB, and Edwards C. Adaptive continuous higher order sliding mode control of air breathing hypersonic missile for maximum target penetration. In: *AIAA guidance, navigation, and control conference*, Kissimmee, FL, 5–9 January 2015.
7. Fan YH, Yu YF, and Li X. Design of composite control system for an air-breathing hypersonic vehicle with wing-rudder deflection. *Appl Mech Mater* 2015; 719: 365–368.
8. Spravka JJ and Jorris TR. Current hypersonic and space vehicle flight test and instrumentation. In: *AIAA flight testing conference*, Dallas, TX, 22–26 June 2015.
9. Chavez FR and Schmidt DK. Analytical aeropropulsive/aeroelastic hypersonic-vehicle model with dynamic analysis. *J Guid Control Dynam* 1994; 17(6): 1308–1319.
10. Kelkar A, Vogel J, Whitmer C, et al. Design tool for control-centric modeling, analysis, and trade studies for hypersonic vehicles. In: *17th AIAA international space planes and hypersonic systems and technologies conference*, San Francisco, CA, 11–14 April 2011.
11. Bolender MA and Doman DB. Nonlinear longitudinal dynamical model of an air-breathing hypersonic vehicle. *J Spacecraft Rockets* 2007; 44(2): 374–387.
12. Matthew K.Adaptive control of an aeroelastic airbreathing hypersonic cruise vehicle. In: *AIAA guidance, navigation and control conference and exhibit*, Hilton Head, SC, 20–23 August 2007.
13. Xu B, Huang X, Wang D, et al. Dynamic surface control of constrained hypersonic flight models with parameter estimation and actuator compensation. *Asian J Control* 2014; 16(1): 162–174.
14. Xu B. Robust adaptive neural control of flexible hypersonic flight vehicle with dead-zone input nonlinearity. *Nonlin Dynam* 2015; 80(3): 1509–1520.
15. Xu B, Wang S, Gao D, et al. Command filter based robust nonlinear control of hypersonic aircraft with magnitude constraints on states and actuators. *J Intell Robot Syst* 2014; 73(1–4): 233–247.
16. Xu B, Guo Y, Yuan Y, et al. Fault tolerant control using command filtered adaptive back-stepping technique: application to hypersonic longitudinal flight dynamics. *Int J Adapt Control Signal Process* 2016; 30(4): 553–577.
17. Fiorentini L, Serrani A, Bolender MA, et al. Nonlinear robust/adaptive controller design for an air-breathing hypersonic vehicle model. In: *The proceedings of the 2007 AIAA guidance, navigation and control conference and exhibit*, Hilton Head, South Carolina, 20–23 August 2007.
18. Xu H, Mirmirani MD, and Ioannou PA. Adaptive sliding mode control design for a hypersonic flight vehicle. *J Guid Control Dynam* 2004; 27(5): 829–838.
19. Fan YH, Yan PP, Wang F, et al. Discrete sliding mode control for hypersonic cruise missile. *Discrete Dyn Nat Soc*, 24 March 2016, 38(6).
20. Xu B, Zhang Q, and Pan Y. Neural network based dynamic surface control of hypersonic flight dynamics using small-gain theorem. *Neurocomputing* 2016; 173: 690–699.
21. Xu B, Yang C, and Pan Y. Global neural dynamic surface tracking control of strict-feedback systems with application to hypersonic flight vehicle. *IEEE Trans Neural Netw Learn Syst* 2015; 26(10): 2563–2575.
22. Xu B, Gao D, and Wang S. Adaptive neural control based on HGO for hypersonic flight vehicles. *Sci China Inf Sci* 2011; 54(3): 511–520.
23. Xu B, Fan Y, and Zhang S. Minimal-learning-parameter technique based adaptive neural control of hypersonic flight dynamics without back-stepping. *Neurocomputing* 2015; 164: 201–209.

24. Holland SD, Woods WC, and Engelund WC. Hyper-X research vehicle experimental aerodynamics test program overview. *J Spacecraft Rockets* 2001; 38(6): 828–835.
25. Clarks A, Wu C, Mirmiranit M, et al. Development of an airframe-propulsion integrated generic hypersonic vehicle model. *In:* 44th AIAA aerospace sciences meeting and exhibit*, Reno, NV, 9–12* January 2006.
26. Mracek CP and Ridgely DB. Missile longitudinal autopilots: connections between optimal control and classical topologies. In: *AIAA guidance, navigation and control conference and exhibit*, San Francisco, California, 15–18 August 2005, pp. 1–29.